Vol.3, No.5, Page 1187- 1194, 2025 https://doi.org/10.59628/jast.v3i5.2320 ISSN 2958-9568 JAST

SUN PUBLISHER

مجلة جامعة صنعاء للعلوم التطبيقية والتكنولوجيا

Sana'a University Journal of Applied Sciences and Technology

https://journals.su.edu.ye/index.php/jast/

A new study on the interaction of structured Laguerre-Bessel-Gaussian beam with a chiral medium

F. Boufalah , L. Dalil-Essakali and A. Belafhal *

Laboratory of Nuclear, Atomic, Molecular Physics, Mechanic and Energetic Laser Physics Group, Department of Physics, Faculty of Sciences, Chouaïb Doukkali University, P. B 20, 24000 El Jadida, Morocco

*Corresponding author: belafhal@gmail.com

Abstract

Using the Huygens-Fresnel diffraction integral, the electric field distribution of the Laguerre-Bessel-Gaussian (LBG) beam in a chiral medium is analytically expressed. The findings demonstrate that the LBG beam is divided into two parts: a right circularly polarized (RCP) beam and a left circularly polarized (LCP) beam. The chiral parameter, wavelength, and orders of the Bessel and Laguerre beams are affected by different propagation trajectories. The left circularly polarized beam was observed to accelerate more quickly than the right circularly polarized beam during propagation, and this acceleration was dependent on the chiral parameter. With an increase in the chiral parameter, the RLP beams decreased, and the LCP beams accelerated. The results of this investigation will be useful in optical manipulation and sorting applications.

Article Info

Keywords:
Propagation, Right circularly polarized beams, Chiral medium, Left circularly polarized beams

Article History:
Received: 03-October-2025,
Revised: 20-October -2025,
Accepted: 23-October -2025,
Available online: 28 October 2025.

1. INTRODUCTION

as a solution to the paraxial wave equation in cylindrical coordinates, Tovar [1] introduces the LBG beam. This type of beam can be regarded as a hybrid mode that combines features from both Bessel-Gaussian (BG) and Laguerre- Gaussian (LG) beams. Specifically, the LBG beam exhibits the radial confinement and nondiffracting nature of the BG beams, along with the azimuthal phase structure and orbital angular momentum properties of LG beams. These combined characteristics make the LBG beam particularly attractive for structured light applications. In addition to being representable by ABCD matrices, these solutions are valid for electromagnetic waves propagating through circularly symmetric optical systems and across open spaces. Mei and Zhao [2] used Rayleigh-Sommerfeld vector formulas to study the nonparaxial propagation of LBG vector beams, and Saad et al. [3]used the Fresnel integral formula to study the propagation of an LBG beam through a helical axicon. Generalized Bessel-Laguerre-Gaussian beams were presented by our research team as new solutions to the paraxial wave equation in cylindrical coordinates. Boufalah et al [4, 5] studied the average axial intensity of the propagation of a generalized Bessel-Laguerre-Gaussian beam through a turbulent atmosphere and the approximate analytical expression of diffraction of a generalized Bessel-Laguerre-Gaussian beam passing through an ABCD optical system. The investigation of several chiral medium-propagating structured light beams has been of great interest in recent years; therefore, it is necessary to examine them. Many characteristics of chiral media differ from those of regular optical media. Chiral media are present in biological materials, such as human tissue, therapeutic materials, and some types of terrestrial vegetation layers [6]. However, when a linearly polarized beam is divided into two circularly polarized beams, the (LCP) beam and the (RCP) beam, when it impacts a chiral material [6–8]. Numerous reports exist about beam propagation through chiral media, Zhuang et al. [7] explore the characteristics of an Airy beam propagating in a chiral material, the analytical expressions of electric field distribution of the vortex Airy beam through an optical ABCD system of a chiral medium

are treated by Liu et Zhao [8], Deng et al. [9] study an Airy beam's characteristics across a chiral material and Hua et al. [10] introduce the Airy-Gaussian Vortex beam propagation in a chiral media both theoretically and statistically. Additionally, the intensity, phase, and gradient force distributions of chirped-Airy-Gaussian vortex beams propagating in the chiral media have been examined by Zhou et al. [11], Xie et al. [12] have investigated how the propagation of Airy vortex beams is affected by the chiral and first-order chirped parameters and using the ABCD transfer matrix and Collins formula, Hui et al. [13] investigated the dynamical properties and propagation of a Bessel–Gaussian beam in a chiral medium. More recently, Hricha et al. [14] studied cosine-hyperbolic-Gaussian beams propagating paraxially in a chiral medium, and paraxial propagation of Hermite cosine-hyperbolic-Gaussian beams treated by Yaalou et al. [15]. Qiu and Liu [16] investigated the Transmission of Tricomi-Gaussian beams in a chiral medium, and examined the properties of generalized Hermite cosh-Gaussian beams traveling in a chiral medium by Saad et al. [17]. Benzehoua et al. [18] derived Laguerre higher-order cosh-Gaussian beam's paraxial propagation characteristics through a chiral medium, and investigated the orbital angular momentum light beam propagation properties through a chiral medium by Razzaz and Arfan [19]. In this study, the propagation properties of a non-diffracting LBG beam in a chiral medium were investigated using the Huygens-Fresnel diffraction integral formula. The remainder of this paper is organized as follows. In Section 2, we derive the propagation expression of the LBG beam through an ABCD optical system. Section 3 extends this analysis to a chiral medium, where we investigate the influence of the chirality parameter on beam evolution. Section 4 discusses particular propagation cases, and Section 5 presents detailed numerical simulations demonstrating the asymmetric acceleration of the left- and right-circularly polarized (LCP/RCP) components. The results show that increasing the chiral parameter leads to stronger beam deflection and enhanced focusing of the LCP beams. Finally, the main findings and potential implications are summarized in Section 6.

2. EVOLUTION OF A LBG BEAM THROUGH AN ABCD OPTICAL SYSTEM

In a cylindrical coordinate system, the field distribution of the initial plane, the LBG beam, can be expressed as follows [1]:

$$u_0(r_0,\varphi_0,0)=\left(\frac{\sqrt{2}\,r_0}{\omega_0}\right)^m L_n^m\left(\frac{2r_0^2}{\omega_0^2}\right) J_q\left(\frac{\alpha r_0}{\omega_0}\right) \times \exp\left(-\frac{r_0^2}{\omega_0^2}\right)\exp(i(q-m)\varphi_0). \tag{1}$$

In this definition, $L_n^{(m)}$ is the Laguerre polynomial of orders m and n, (r_0,φ_0) are the cylindrical coordinates with $r_0=\sqrt{x_0^2+y_0^2}$ and $\varphi_0=\tan^{-1}\left(\frac{y_0}{x_0}\right)$ are the phase angle (x_0,y_0) is the Cartesian coordinate, J_q is the q th-order Bessel function of the first kind, ω_0 is the radius of the beam waist, $\frac{\alpha}{\omega_0}=k_0\sin\beta$ is the transverse wave number with $k_0=\frac{2\pi}{\lambda_0}$ is the wave number of the beam in free space, λ_0 is the wavelength, and β is the half-cone angle of the beam. We used the Collins diffraction integral formula to determine the evolution of the LBG beam using an ABCD optical system. The output field is expressed as follows:

$$u(r,\phi,z)=-\frac{ik_0}{2\pi B}\int_0^\infty\int_0^{2\pi} u_0(r_0,\phi_0,0) \times\exp\left\{\frac{ik}{2B}\left[Ar_0^2-2rr_0\cos(\phi_0-\phi)+Dr^2\right]\right\} r_0\,d\phi_0\,dr_0. \tag{2}$$

where A, B, C and D are the elements transfer matrix. Substituting the expression for given by Eq. 1 in Eq. 2, and using the following integral identity [20]:

$$\int_0^{2\pi}\exp\left[-\frac{ikrr_0}{B}\cos(\phi-\phi_0)+i(q+m)\phi_0\right]d\phi_0=2\pi\,(-i)^{q-m} \exp[i(q+m)\phi]\,[4pt] \times J_{q+m}\left(\frac{k_0r_0r}{B}\right). \tag{3}$$

one finds

$$u(r,\phi,z)=\frac{(-i)^{(q-m+1)}\,k_0}{B}\exp\left(\frac{ik_0Dr^2}{2B}\right)\left(\frac{\sqrt{2}}{\omega_0}\right)^m \exp\left[i\,(q-m)\,\phi\right]I, \tag{4}$$

where $I$is expressed as

$$I=\int_0^\infty t^{m+1}\exp\left(-\sigma t^2\right)L_n^{(m)}\left(\frac{2}{\omega_0^2}t^2\right)J_q\left(\zeta t\right)J_{q-m}\left(\varepsilon t\right)dt, \tag{5}$$

with

$$\zeta=\frac{\alpha}{\omega_0}, \tag{6a}$$

$$\varepsilon=\frac{k_0r}{B}, \tag{6b}$$

and

$$\sigma=\frac{1}{\omega_0^2}-\frac{ik_0A}{2B}. \tag{6c}$$

The integral of Eq. 5 can be evaluated by exporting the generalized Laguerre polynomial and Bessel function as follows:

$$L_n^{(m)}\left(z\right)=\frac{(m+1)_n}{n!}\sum_{p=0,n}\frac{(-n)_p}{(m+1)_p}\frac{z^p}{p!}, \tag{7}$$

and

$$J_\nu\left(z\right)=\sum_{s=0,\infty}\frac{(-1)^s\left(\frac{z}{2}\right)^{\nu+2s}}{s!\Gamma\left(\nu+s+1\right)}. \tag{8}$$

After tedious algebraic manipulations, using the above equations and the integral identity Eq.6.633 of [20], Eq. 5 can be established as

$$I = \frac{\zeta^q \varepsilon^{q-m}}{2^{2q+1-m}\sigma^{q+1} q!} \sum_{p=0}^{n} \frac{\Gamma(n+m+1)}{p!\,\Gamma(n-p+1)\,\Gamma(m+p+1)} \left(-\frac{2}{\omega_0^2\sigma}\right)^p \times \sum_{s=0}^{\infty} \frac{\Gamma(s+p+q+1)}{s!\,\Gamma(s+q-m+1)} \left(-\frac{\zeta^2}{4\sigma}\right)^s {}_2F_1\left(-s,\, m-q-s;\, q+1;\, \frac{\zeta^2}{\varepsilon^2}\right). \tag{9}$$

where ${}_2F_1$ is the hypergeometric series given by

$${}_2F_1\,(a,b;c;z) = \sum_{l=0}^{\infty} \frac{(a)_l\,(b)_l}{(c)_l} \frac{z^l}{l!}. \tag{10}$$

Therefore, the Collins formula (Eq. 2 gives the output fields, which can be written as

$$\begin{aligned} u(r,\varphi,z) = {} & \frac{(-i)^{q-m+1}k_0}{2B\sigma\, q!} \exp\left(\frac{ik_0 D r^2}{2B}\right) \left(\frac{2\sqrt{2}}{\omega_0\varepsilon}\right)^m \left(\frac{\zeta\varepsilon}{4\sigma}\right)^q \\ & \times \sum_{p=0}^{n} \frac{\Gamma(n+m+1)\left(-\dfrac{2}{\omega_0^2\sigma}\right)^p}{\Gamma(n-p+1)\Gamma(m+p+1)p!} \\ & \times \exp[i(q-m)\varphi] \\ & \times \sum_{s=0}^{\infty} \frac{\Gamma(s+p+q+1)}{\Gamma(s+q-m+1)} \frac{\left(-\dfrac{\varepsilon^2}{4\sigma}\right)^s}{s!} \\ & \times {}_2F_1\left(-s,\, m-q-s;\, q+1;\, \frac{\zeta^2}{\varepsilon^2}\right) \end{aligned} \tag{11}$$

This equation is our first main result that shows the evolution of the LBG beam propagating through the ABCD optical system. Note that from this expression, one car easily evolves the following beams: By taking $n = m = 0$, Eq. 11 becomes the output field corresponding to a Bessel-Gaussian beam. In this case, we assume $\alpha = 0$ and $(n,m) \neq (0,0)$. In the following section, we apply Eq. 11 for a chiral medium.

3. THE LBG BEAM'S PROPAGATION THROUGH A CHIRAL MEDIUM

This medium characterized by the ABCD transfer matrix expressed as [21]

$$\begin{bmatrix} A & B_L \\ C & D \end{bmatrix} = \begin{bmatrix} 1 & \frac{z}{n_L} \\ 0 & 1 \end{bmatrix}, \tag{12a}$$

and

$$\begin{bmatrix} A & B_R \\ C & D \end{bmatrix} = \begin{bmatrix} 1 & \frac{z}{n_R} \\ 0 & 1 \end{bmatrix}. \tag{12b}$$

where $n_R = \frac{n_0}{1-n_0k_0\gamma}$ and $n_L = \frac{n_0}{1+n_0k_0\gamma}$ are the refractive indices of the RCP and LCP beams, respectively. In these expressions, γ represents the chiral parameter and $n_0$indicates the original refractive index of the chiral medium. The ABCD matrices for the RCP and LCP beams differ, as shown in Equation 12. By the use of Eqs. 11 and 12, the analytical expression of the LBG beam in the chiral medium can be written as

$$u^{L,R}(r,\varphi,z) = u_0^{L,R}(r)\;\; u_{m,q}^{L,R}(r,\varphi,z), \tag{13}$$

where

$$u_0^{L,R}(r) = \frac{k_0}{2\sigma B} \exp\left(\frac{ik_0}{2B} r^2\right), \tag{14}$$

and

$$\begin{aligned} u_{m,q}^{L,R}(r,\varphi,z) = {} & \frac{(-i)^{q-m-1}}{q!} \left(\frac{2\sqrt{2}\,B}{\omega_0 k_0 r}\right)^m \left(\frac{\alpha k_0}{4\omega_0\sigma B} r\right)^q \\ & \times \exp\left(i(q-m)\varphi\right) \\ & \times \sum_{p=0}^{n} A_p(m,n) \sum_{s=0}^{\infty} B_s(p,q,m)\, r^{2s} \\ & \times {}_2F_1\left(-s, m-q-s; q+1; \frac{R}{r^2}\right), \end{aligned} \tag{15}$$

with

$$\Re = \frac{\alpha^2 B^2}{\omega_0^2 k_0^2} \tag{16a}$$

$$A_p(m,n) = \frac{\Gamma(n+m+1)}{\Gamma(n-p+1)\,\Gamma(m+p+1)} \frac{\left(-\frac{2}{\sigma\omega_0^2}\right)^p}{p!} \tag{16b}$$

and

$$B_s(p,q,m) = \frac{\Gamma(s+p+q+1)}{\Gamma(s+q-m+1)} \frac{\left(-\frac{k_0^2}{4\sigma B^2}\right)^s}{s!} \tag{16c}$$

In Eqs. 16, B is given by $B_L = \frac{z}{n_0}(1+k\gamma)$ and$B_R = \frac{z}{n_0}(1-k\gamma)$for the two-component LCP and RCP beams in the chiral medium, respectively. Where $k = n_0k_0$ is the wavenumber of the LBG beam. Consequently, the total electric field can be evaluated using Eqs. 15-16.

$$\begin{aligned} E(r,\phi,z) = {} & u^L(r,\phi,z) \exp\left(\frac{ik_0n_0}{1+n_0k_0\gamma} z\right) \\ & + u^R(r,\phi,z) \exp\left(\frac{ik_0n_0}{1-n_0k_0\gamma} z\right). \end{aligned} \tag{17}$$

The total intensity of LBG beam propagation in chiral medium is expressed as

$$I(r,\varphi,z) = \left|u^L(r,\varphi,z)\right|^2 + \left|u^R(r,\varphi,z)\right|^2 + I_{interf}(r,\varphi,z), \tag{18}$$

where I_{interf} the interference term is given by

$$I_{interf}(r,\phi,z) = u^{L}(r,\phi,z)\,u^{R*}(r,\phi,z)\exp\left[i\left(k_L-k_R\right)z\right] + u^{L*}(r,\phi,z)\,u^{R}(r,\phi,z)\exp\left[-i\left(k_L-k_R\right)z\right], \tag{19}$$

whit * represents the superscript.

4. PARTICULAR CASES

In this section, we investigate two important cases of Laguerre-Gaussian and Bessel-Gaussian beams, which can be deduced from our main result in Eq. 4.

4.1. LAGUERRE-GAUSSIAN BEAM PROPAGATING THROUGH A CHIRAL MEDIUM

By using the series of generalized Laguerre polynomials given by Eq. 7, and the Bessel function in Eq. 8, one finds the following identity

$$\begin{aligned}\int_0^{\infty} x^{2\gamma+1}\exp\left(-\sigma x^2\right)L_n^{(\alpha)}\left(\eta x^2\right)J_\nu(\mu x)\,dx &= \frac{\mu^{\nu}\Gamma(n+\alpha+1)}{2^{\nu+1}\sigma^{\frac{\nu}{2}+\gamma+1}}\exp\left(-\frac{\mu^2}{4\sigma}\right)\\ &\times\sum_{p=0}^{n}\frac{\Gamma\left(\gamma+p+1-\frac{\nu}{2}\right)}{\Gamma(n-p+1)\Gamma(\alpha+p+1)}\frac{\left(-\frac{\eta}{\sigma}\right)^p}{p!}\\ &\times L_{p+\gamma-\frac{\nu}{2}}^{(\nu)}\left(\frac{\mu^2}{4\sigma}\right)\end{aligned} \tag{20}$$

Using this identity, Eq. 5 can be rewritten, in this case, as

$$\begin{aligned}\int_0^{\infty} x^{m+1}\exp\left(-\sigma x^2\right)L_n^{(m)}\left(\eta x^2\right)J_\nu(\mu x)\,dx &= \left(\frac{\varepsilon}{2}\right)^m\frac{(m+1)_n}{2}\exp\left(-\frac{\varepsilon^2}{4\sigma}\right)\\ &\times\sum_{p=0}^{n}\frac{\left(-\frac{\eta}{\sigma}\right)^p}{\Gamma(n-p+1)\,\Gamma(m+p+1)}\\ &\times L_p^{(m)}\left(\frac{\varepsilon^2}{4\sigma}\right)\end{aligned} \tag{21}$$

And consequently, the output field is expressed as

$$\begin{aligned}u^{L,G}(r,\varphi,z) = \frac{-ik_0}{2B}(m+1)_n\left(\frac{\varepsilon}{i\sqrt{2}\,\omega_0}\right)^m\exp(-im\varphi)\\ \times\exp\left[-\left(\frac{k_0^2}{2\sigma B}-ik_0D\right)\frac{r^2}{2B}\right]\\ \times\sum_{p=0}^{n}\frac{\left(\frac{-\eta}{\sigma}\right)^p}{\Gamma(n-p+1)\,\Gamma(m+p+1)}L_p^{(m)}\left(\frac{\varepsilon^2}{4\sigma}\right).\end{aligned} \tag{22}$$

One can see from Eq. 22, the resulting field of the ABCD optical system is a finite superposition of Laguerre-Gaussian beams with some amplitude phases. For the propagation of this beam through a chiral medium, it's easy to introduce in Eq. 22, the matrix elements are $D = 1$ and$B$. This last element has two components: $B_L = \frac{z}{n_0}(1+k\gamma)$ and. $B_R = \frac{z}{n_0}(1-k\gamma)$.

4.2. PROPAGATION OF BESSEL-GAUSSIAN BEAM THROUGH A CHIRAL MEDIUM

For the evolution of the output field, $u^{B,G}(r,\varphi,z)$, which is given by Eq. 4, we recall the identity 6.633 of [20], given by:

$$\begin{aligned}\int_0^{\infty} xe^{-\sigma x^2}J_q(\mu x)J_q(\lambda x)\,dx = \frac{\mu^{\nu}\lambda^{\chi}}{2^{\nu+\chi+1}\,\Gamma\left(\frac{\nu+\chi}{2}+\gamma+1\right)\nu!}\\ \times\sum_{s=0}^{\infty}\frac{\Gamma\left(s+\frac{\nu+\chi}{2}+\gamma+1\right)}{s!\,\Gamma(s+\chi+1)}\left(-\frac{\lambda^2}{4\sigma}\right)^s\\ \times\,{}_2F_1\left(-s,-\chi-s;\nu+1;\frac{\mu^2}{\lambda^2}\right).\end{aligned} \tag{23}$$

with $Re(\sigma) > 0$and $Re(2\gamma+\chi+\nu) > -2$; $\lambda > 0$and$\mu > 0$. By taking $\gamma = 0$and $\nu = q = \chi$, Eq. 23 becomes

$$\begin{aligned}\int_0^{\infty} x\,e^{-\sigma x^2}J_q(\mu x)\,J_q(\lambda x)\,dx = \frac{1}{2\sigma\,q!}\left(\frac{\mu\lambda}{4\sigma}\right)^q\\ \times\sum_{s=0}^{\infty}\frac{\left(-\frac{\lambda^2}{4\sigma}\right)^s}{s!}\,{}_2F_1\left(-s,-\chi-s;\nu+1;\frac{\mu^2}{\lambda^2}\right)\end{aligned} \tag{24}$$

The last equation can be rewritten using Eq. 12 of Ref. [22] given by

$$\begin{aligned}\int_0^{\infty} x\,e^{-\sigma x^2}J_q(\mu x)\,J_q(\lambda x)\,dx = \frac{(-1)^q}{2\sigma}\exp\left(iq\frac{\pi}{2}\right)\exp\left[-\frac{\mu^2+\lambda^2}{4\sigma}\right]\\ \times J_q\left(i\frac{\mu\lambda}{2\sigma}\right).\end{aligned} \tag{25}$$

In the case of $\lambda = 2$ and $\mu = \zeta$, one can deduce the following identity

$$\begin{aligned}\sum_{s=0}^{\infty}\frac{\left(-\frac{\lambda^2}{4\sigma}\right)^s}{s!}\,{}_2F_1\left(-s,-\chi-s;\nu+1;\frac{\mu^2}{\lambda^2}\right) = q!\left(-\frac{4\sigma}{\zeta\varepsilon}\right)^q\exp\left(iq\frac{\pi}{2}\right)\\ \times\exp\left[-\frac{\zeta^2+\varepsilon^2}{4\sigma}\right]J_q\left(i\frac{\zeta\varepsilon}{2\sigma}\right)\end{aligned} \tag{26}$$

Finally, Eq. 4 can be writter, in this case, as

$$\begin{aligned}u^{B,G}(r,\phi,z) = \frac{k_0i^q}{2\sigma B}\exp\left(\frac{ik_0D}{2B}r^2\right)\exp\left[iq\left(\phi+\frac{\pi}{2}\right)\right]\\ \exp\left[-\frac{(\zeta^2+\varepsilon^2)}{4\sigma}\right]J_q\left(i\frac{\zeta\varepsilon}{2\sigma}\right).\end{aligned} \tag{27}$$

From this expression,,, and Eq. 12, the total electric field propagation in a chiral medium can be determined. Our results are the same as those obtained using Eq. 6 of Ref. [13].

5. NUMERICAL SIMULATIONS

The following parameters were used in the calculations:$\lambda = 632.8nm$,$\omega_0 = 0.06\lambda$,$z_0 = 0.02\mu m$, and $n_0 = 3$. Figs.1(a1–a3) display the evolution of the LBG beam through the chiral medium with the chirality parameter $\mathrm{fl} = 0.1/\mathrm{k}_0$. A clear asymmetry was observed in the propagation trajectories of the left- and right-circularly polarized (LCP and RCP) components, as shown in Figs. 1(a1) and (a2). Specifically, the LCP beam diverged and diffracted more rapidly than the RCP beam did. This behavior stems from the optical activity of the chiral medium, which introduces different effective refractive indices for the two polarizations, owing to their opposite spin angular momenta. Stronger coupling between the LCP component and handedness of the medium leads to enhanced phase accumulation and spatial spreading. Fig. 1(a3) shows the total intensity distribution of the beam, where the interference effects and polarization asymmetry cause noticeable distortions. When the chirality parameter increases to $\mathrm{fl} = 0.5/\mathrm{k}_0$, as shown in Figs. 1(b1–b3), the difference in divergence between the LCP and RCP beams is further accentuated, yet the overall divergence of the total intensity profile is reduced. This suggests a nonlinear relationship between the beam separation and global beam confinement, offering a degree of tunability. These results indicate that the chirality parameter γ can serve as a control knob for tailoring the spatial evolution of structured beams. Such control can be leveraged in polarization-sensitive beam steering, optical sorting of chiral particles, and information encoding in optical communication systems, where manipulating the beam trajectory via polarization offers selective and dynamic routing capabilities.

The results in Fig.1 are qualitatively consistent with those reported by Hui et al. [13], where the Bessel–Gaussian beam components, LCP and RCP, propagate differently in a chiral medium. However, owing to the specific structure of the LBG beam, a more pronounced deformation of the total intensity was observed, especially as the chirality parameter γ increased. This difference highlights the richer spatial dynamics offered by the LBG beam, which combines both the Bessel and Laguerre-type structures. Fig. 2 displays the intensity distribution of the LBG beam propagating in the chiral medium during the effects of two γ values in the near and far zones.

In this figure, we can observe that the LCP and RCP beams are not significantly affected by the various chiral parameters in the near and far zones, but the interference beams and the total beams are affected when $\gamma$and z increase. It can be seen that the intensity is always mirror symmetric for low and high propagation distances z, and the number of side-lobes accompanying the central lobe does not change; however, its

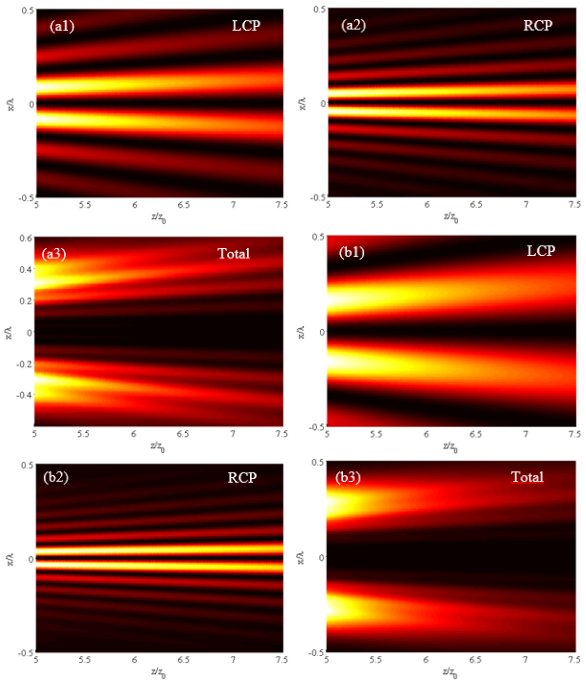

Figure 1. Propagation of the LBG beam's intensity in the chiral medium with $\mathrm{q} = 3,\beta = 10°$and $\mathrm{m} = 4.(\mathrm{a1}) - (\mathrm{a3})\ \gamma = 0.1/k_0$ and $(\mathrm{b1}) - (\mathrm{b3})\ \gamma = 0.5/k_0$.

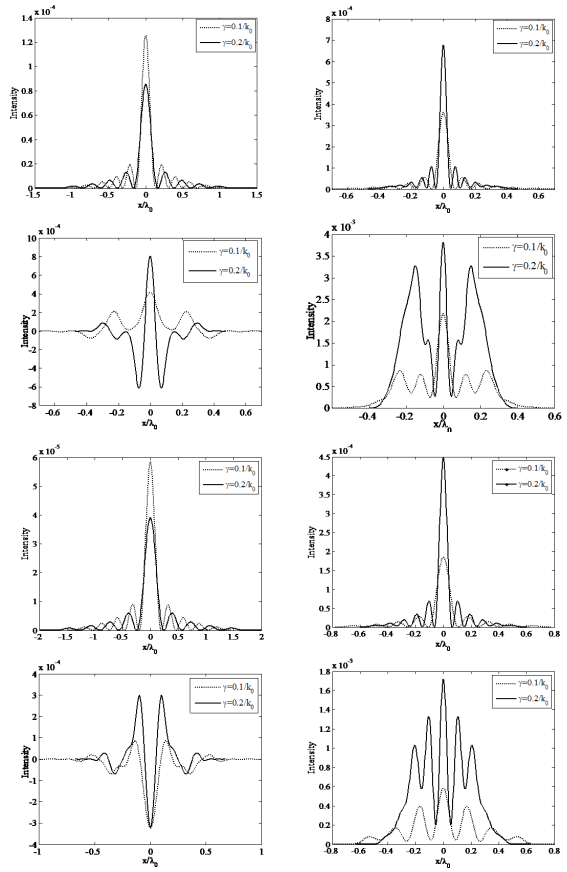

Figure 2. The LBG beam's propagation intensity distribution in the chiral medium with $\mathrm{q} = 2,\ \alpha = 15°,\mathrm{m} = 2.(\mathrm{a1}) - (\mathrm{a2})\ \mathrm{z} = 0.1\mu m$ and $(\mathrm{b1}) - (\mathrm{b2})\ \mathrm{z} = 0.15\mu m$.

distribution in the x-direction is most important if z increases. The normalized intensity distribution of the LCP and RCP beams on the (x, y) plane with varying beam order numbers q and two values for the chiral parameters ($\mathrm{fl} = 0.1/\mathrm{k_0}and\mathrm{fl} = 0.5/\mathrm{k_0}$) at distance z is shown in Fig. 3.

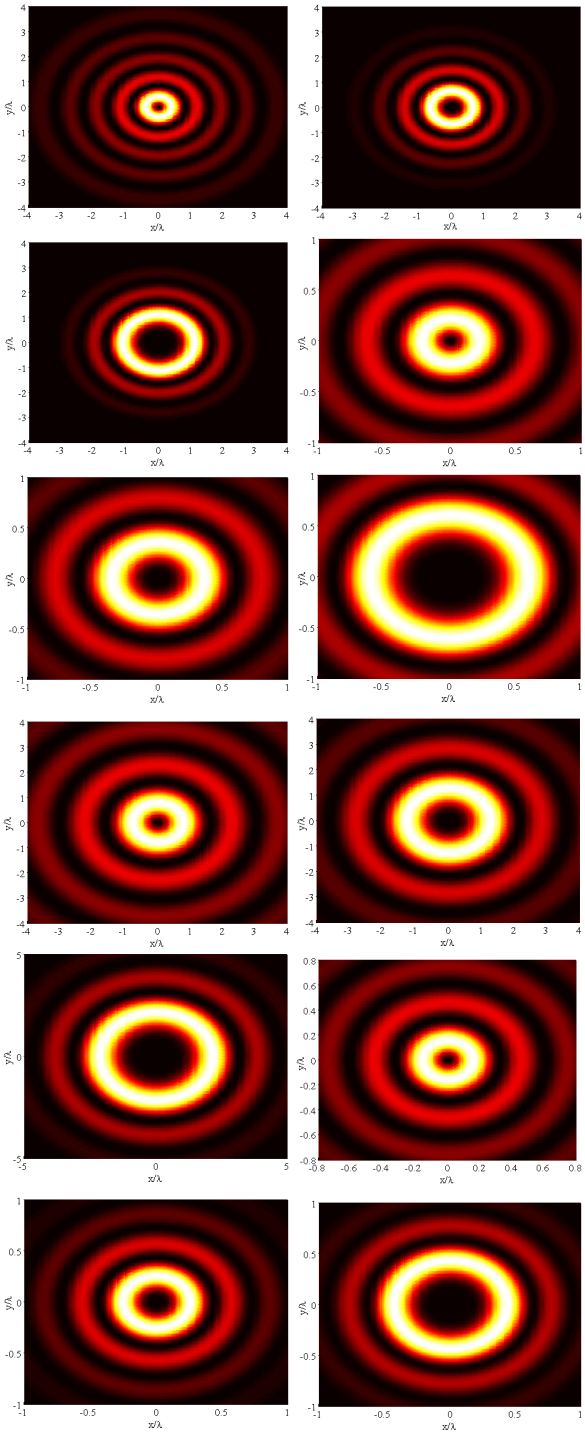

Figure 3. Intensity of the LCP and RCP beam propagating through the chiral medium with$\mathrm{z} = 0.4\mu\mathrm{m}$,$\beta = 15°$,$\mathrm{m} = 4$.

It is evident from this figure that as the chiral parameter $\gamma$and beam order number q increase, so does the radius of the central dark area of the LBG beam traveling through the chiral medium. We can also observe that the central dark area of the LCP is larger than that of the RCP. The first and third lines represent the LCP light-normalized intensity, and the second and fourth lines denote the RCP light-normalized intensity. $(\mathrm{a1}) - (\mathrm{a3}), (\mathrm{b1}) - (\mathrm{b3})\,\mathrm{fl} = 0.1/\mathrm{k_0}$ and $(\mathrm{c1}) - (\mathrm{c3}), (\mathrm{d1}) - (\mathrm{d3})\,\mathrm{fl} = 0.5/\mathrm{k_0}$. Fig. 4 illustrates the phase distributions of the LCP component of the LBG beam propagating through a chiral medium with two values of the chiral parameter γ at the distance $\mathrm{z} = 0.1\mu\mathrm{m}$, and varying beam order number q were examined, as shown in Fig. 4. We can see that the phase pattern

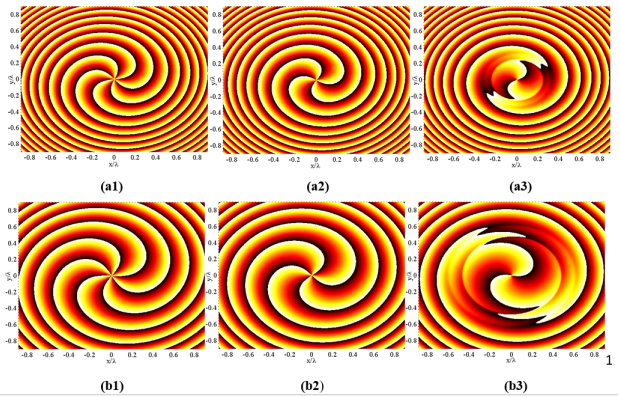

Figure 4. Phases of the LCP beam propagation in the chiral medium with $\mathrm{z} = 0.1\mu\mathrm{m}$,$\beta = 50°$ and $\mathrm{m} = 6$.$(\mathrm{a1}) - (\mathrm{b1})\ \mathrm{q} = 0$,$(\mathrm{a2}) - (\mathrm{b2})\ \mathrm{q} = 2$ and$(\mathrm{a3}) - (\mathrm{b3})\ \mathrm{q} = 4$. $(\mathrm{a1}) - (\mathrm{a3})\ \mathrm{fl} = 0.1/\mathrm{k_0}$ and $(\mathrm{b1}) - (\mathrm{b3})\ \mathrm{fl} = 0.5/\mathrm{k_0}$.

exhibits a spiral modality and always rotates in the clockwise direction when q and γ increase. It is also clear that the phase pattern at $\mathrm{fl} = 0.1/\mathrm{k_0}$ shows a higher degree of convergence at $\mathrm{fl} = 0.5/\mathrm{k_0}$. Additionally, there is a notable difference in the vortex properties and behaviors at beam order number q=4. Fig. 5 illustrates the phase distributions of the RCP (a1–a3) and LCP (b1–b3) components of the LBG beam as they propagate through a chiral medium at three different wavelengths. The simulation parameters were fixed as follows: $\mathrm{z} = 0.1\mu\mathrm{m}$,$\beta = 50°$, $\mathrm{fl} = 0.5/\mathrm{k_0}$,$\mathrm{q} = 2$, and $\mathrm{m} = 6$. The phase profiles show clear spiral structures for both polarizations. As the wavelength increased, the spirals became more compact, and the phase fringes became denser. This behavior results from the inverse dependence of the wavenumber $k_0 = \frac{2\pi}{\lambda_0}$, which increases the effective chiral parameter $\mathrm{fl} = 0.5/\mathrm{k_0}$at longer wavelengths. Consequently, the optical activity becomes stronger, leading to a tighter phase winding and steeper gradients. These effects were evident in both the RCP and LCP components, with noticeable modifications in the phase concentration and topology, especially at $\lambda = 800nm$.

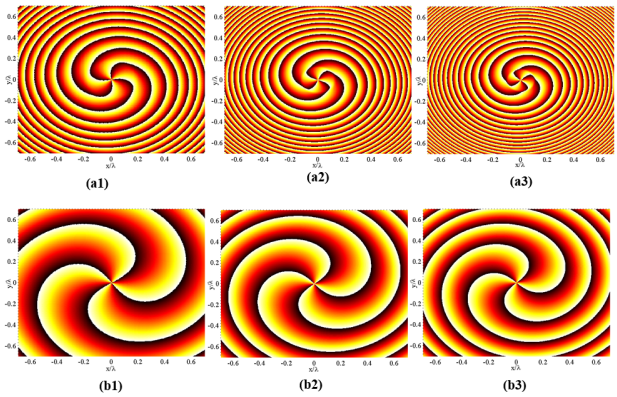

Figure 5. Phases of the RCP beam and the LCP beam propagation in the chiral medium with $z = 0.1\mu m$,$\beta = 50°$, $fl = 0.5/k_0$, $q = 2$ and $m = 6$.(a1) and (b1) $\lambda = 400nm$, (a2) and (b2) $\lambda = 632.8nm$, and (a3) and (b3) $\lambda = 800nm$. $(a1) - (a3)$ are the RCP phase distributions and $(b1) - (b3)$ are the LCP phase distributions.

6. CONCLUSION

In this study, we used the Huygens diffraction integral to theoretically and numerically study the propagation of an LBG beam in a chiral medium. We also demonstrate that the LBG beam is divided into two components with differing propagation trajectories: the LCP and RCP beams, both of which are affected by the chiral parameter γ, distance of propagation z, beam order number q, and wavelength. In addition, it was found that the LCP beams accelerated faster than the RCP beams during propagation. Therefore, these characteristics of GBL beam propagation make it a strong contender for actual experimental applications such as optical sorting and laser optics.

Declarations

Ethical Approval This article does not contain any studies involving animals or human participants performed by any of the authors. We declare that this manuscript is original and is not currently being considered for publication elsewhere. We further confirm that the order of the authors listed in the manuscript has been approved by all authors.

Competing interests The authors have no financial or proprietary interest in any material discussed in this article. **Authors' contributions** All the authors contributed to the conception and design of the study. All authors performed simulations, data collection, and analysis and commented on the present version of the manuscript. All authors have read and approved the final manuscript.

Funding:

No funding was received from any organization for this study. **Availability of data and materials** No datasets is used in the present study.

Consent for publication The authors confirm that there was informed consent to publish the data contained in the article.

Consent to participate

Informed consent was obtained from all authors.

REFERENCES

[1] A. A. Tovar, "Propagation of laguerre-bessel-gaussian beams," *J. Opt. Soc. Am. A*, vol. 17, no. 11, pp. 2010–2018, 2000. DOI: 10.1364/JOSAA.17.002010.

[2] Z. Mei and D. Zhao, "Nonparaxial analysis of vectorial laguerre-bessel-gaussian beams," *Opt. Express*, vol. 15, no. 19, pp. 11 942–11 951, 2007. DOI: 10.1364/OE.15.011942.

[3] F. Saad, Z. Hricha, M. Khouilid, and A. Belafhal, "A theoretical study of the fresnel diffraction of laguerre-bessel-gaussian beam by a helical axicon," *Optik*, vol. 149, pp. 416–422, 2017. DOI: 10.1016/j.ijleo.2017.09.068.

[4] F. Boufalah, L. Dalil-Essakali, L. Ez-Zariy, and A. Belafhal, "Introduction of generalized bessel-laguerre-gaussian beams and its central intensity travelling a turbulent atmosphere," *Opt. Quantum Electron.*, vol. 50, no. 8, pp. 305–324, 2018. DOI: 10.1007/s11082-018-1573-2.

[5] F. Boufalah, L. Dalil-Essakali, and A. Belafhal, "Transformation of a generalized bessel–laguerre-gaussian beam by a paraxial abcd optical system," *Opt. Quantum Electron.*, vol. 51, no. 8, pp. 274–289, 2019. DOI: 10.1007/s11082-019-1989-3.

[6] F. Zhuang, X. Du, and D. Zhao, "Polarization modulation for a stochastic electromagnetic beam passing through a chiral medium," *Opt. Lett.*, vol. 36, no. 14, pp. 2683–2685, 2011. DOI: 10.1364/OL.36.002683.

[7] F. Zhuang, X. Du, Y. Ye, and D. Zhao, "Evolution of airy beams in a chiral medium," *Opt. Lett.*, vol. 37, no. 11, pp. 1871–1873, 2012. DOI: 10.1364/OL.37.001871.

[8] X. Liu and D. Zhao, "Propagation of a vortex airy beam in chiral medium," *Opt. Commun.*, vol. 321, pp. 6–10, 2014. DOI: 10.1016/j.optcom.2014.01.068.

[9] F. Deng, W. Yu, J. Huang, R. Zhao, J. Lin, and D. Deng, "Propagation of airy-gaussian beams in a chiral medium," *The Eur. Phys. J. D*, vol. 70, no. 4, pp. 87–93, 2016. DOI: 10.1140/epjd/e2016-60677-8.

[10] S. Hua, Y. Liu, H. Zhang, L. Tang, and Y. Feng, "Propagation of an airy-gaussian-vortex beam in a chiral medium," *Opt. Commun.*, vol. 388, pp. 29–37, 2017. DOI: 10.1016/j.optcom.2016.11.001.

[11] K. Zhou et al., "Propagation of the chirped-airy-gaussian-vortex beams in the chiral medium," *J. Opt.*, vol. 20, no. 7, pp. 075 601–075 615, 2018. DOI: 10.1088/2040-8986/aac4c6.

[12] J. Xie et al., "Paraxial propagation of the first-order chirped airy vortex beams in a chiral medium," *Opt. Express*, vol. 26, no. 5, pp. 5845–5856, 2018. DOI: 10.1364/OE.26.005845.

[13] Y. Hui, Z. Cui, Y. Li, W. Zhao, and Y. Han, "Propagation and dynamical characteristics of a bessel-gaussian beam in a chiral medium," *J. Opt. Soc. Am. A*, vol. 35, no. 8, pp. 1299–1305, 2018. DOI: 10.1364/JOSAA.35.001299.

[14] Z. Hricha, M. Lazrek, and A. Belafhal, "Paraxial propagation of cosine-hyperbolic-gaussian beams in a chiral medium," *J. Mod. Opt.*, vol. 69, no. 20, pp. 1159–1169, 2022. DOI: 10.1080/09500340.2022.2160024.

[15] M. Yaalou, Z. Hricha, and A. Belafhal, "Paraxial propagation of hermite cosine-hyperbolic-gaussian beams in a chiral medium," *Opt. Quantum Electron.*, vol. 55, no. 14, pp. 1281–1297, 2023. DOI: 10.1007/s11082-023-05585-z.

[16] Y. Qiu and Z. Liu, "Propagation of tricomi-gaussian beams in a chiral medium," *Results Phys.*, vol. 58, pp. 107 457–107 466, 2024. DOI: 10.1016/j.rinp.2024.107457.

[17] F. Saad, H. Benzehoua, and A. Belafhal, "Study on the characteristics of a generalized hermite cosh-gaussian beams propagating through a chiral medium," *Opt. Quantum Electron.*, vol. 56, no. 7, pp. 1139–1156, 2024. DOI: 10.1007/s11082-024-07070-7.

[18] H. Benzehoua, F. Saad, A. A. A. Ebrahim, and A. Belafhal, "Paraxial propagation properties of a laguerre higher order cosh-gaussian beam passing through a chiral medium," *Opt. Quantum Electron.*, vol. 56, no. 8, pp. 1316–1326, 2024. DOI: 10.1007/s11082-024-07257-y.

[19] F. Razzaz and M. Arfan, "Study of propagation characteristics of light beam with orbital angular momentum (oam) through a chiral medium," *Photonics*, vol. 12, no. 4, pp. 317–332, 2025. DOI: 10.3390/photonics12040317.

[20] I. S. Gradshteyn and I. M. Ryzhik, *Tables of Integrals, Series, and Products*, 5th. New York: Academic Press, 1994.

[21] E. Bahar, "Relationships between optical rotation and circular dichroism and elements of the mueller matrix for natural and artificial chiral materials," *J. Opt. Soc. Am. B*, vol. 25, no. 2, pp. 218–222, 2008. DOI: 10.1364/JOSAB.25.000218.

[22] Y. Cai and X. Lü, "Propagation of bessel and bessel-gaussian beams through an unapertured or apertured misaligned paraxial optical systems," *Opt. Commun.*, vol. 274, no. 1, pp. 1–7, 2007. DOI: 10.1016/j.optcom.2007.01.058.